Biomechanical Rupture Risk Assessment
A Consistent and Objective Decision-Making Tool for Abdominal Aortic Aneurysm Patients

T. Christian Gasser, PhD

KTH Royal Institute of Technology, KTH Solid Mechanics, Stockholm, Sweden

Abstract

Abdominal aortic aneurysm (AAA) rupture is a local event in the aneurysm wall that naturally demands tools to assess the risk for local wall rupture. Consequently, global parameters like the maximum diameter and its expansion over time can only give very rough risk indications; therefore, they frequently fail to predict individual risk for AAA rupture. In contrast, the Biomechanical Rupture Risk Assessment (BRRA) method investigates the wall's risk for local rupture by quantitatively integrating many known AAA rupture risk factors like female sex, large relative expansion, intraluminal thrombus-related wall weakening, and high blood pressure. The BRRA method is almost 20 years old and has progressed considerably in recent years, it can now potentially enrich the diameter indication for AAA repair. The present paper reviews the current state of the BRRA method by summarizing its key underlying concepts (i.e., geometry modeling, biomechanical simulation, and result interpretation). Specifically, the validity of the underlying model assumptions is critically disused in relation to the intended simulation objective (i.e., a clinical AAA rupture risk assessment). Next, reported clinical BRRA validation studies are summarized, and their clinical relevance is reviewed. The BRRA method is a generic, biomechanics-based approach that provides several interfaces to incorporate information from different research disciplines. As an example, the final section of this review suggests integrating growth aspects to (potentially) further improve BRRA sensitivity and specificity. Despite the fact that no prospective validation studies are reported, a significant and still growing body of validation evidence suggests integrating the BRRA method into the clinical decision-making process (i.e., enriching diameter-based decision-making in AAA patient treatment).

Copyright © 2016 Science International Corp.

Problem Definition

Abdominal aortic aneurysm (AAA) disease is a serious condition and causes many deaths, especially in males over 65 years. Progressive treatment (i.e., surgical or endovascular AAA repair) cannot be offered to all patients, and according to the best clinical practice, AAA repair is indicated if rupture risk exceeds the interventional risks. While center-specific treatment risks are reasonably predictable, assessing AAA rupture risk for individual patients remains the bottleneck in clinical decision making. However, an accurate rupture risk assessment is critical to reduce aneurysm- related mortality without substantially increasing the rate of AAA repair.

According to the current clinical practice, AAA rupture risk is assessed by the aneurysm's largest

* Corresponding Author:
T. Christian Gasser, PhD
KTH Royal Institute of Technology
KTH Solid Mechanics
Teknikringen 8D, 1st Floor, room 6360, SE-100 44 Stockholm, Sweden
Tel: +46 8 790 7793; Fax: +46 8 411 2418; E-Mail: gasser@kth.se

transverse diameter and its change over time. Specifically, AAA repair is generally indicated if the largest diameter exceeds 55 mm or if it grows faster than 10 mm per year [1, 2]. The majority of clinicians follow this advice and use both criteria for clinical decision making, see Figure 1. However, this somewhat crude rupture risk assessment is the subject of increasing discussion, and AAAs with a diameters of less than 55 mm can and do rupture (even under surveillance [3]), whereas many aneurysms larger than 55 mm never rupture [4, 5]. Finally, the threshold diameter criterion is already about 20 years old and may no longer adequately reflect current treatment options.

Due to the poor specificity and sensitivity of diameter as an AAA repair indication, the cost-effectiveness of patient treatment for aneurysms is not optimal, and a more individualized AAA repair indication would be of great help. Most important, aneurysm rupture is a *local* failure event in the wall, and *global* parameters like the largest diameter might not adequately reflect the actual risk for such events. This conclusion also explains why not all ruptures are found at the level of the largest diameter. Similarly, monitoring the expansion of the maximum diameter over time lacks sound scientific evidence and also misses spots of fast growth (i.e., areas of potentially compromised wall strength due to incomplete tissue turnover) [6].

The drawbacks of the diameter criterion have stimulated considerable research in the field. Besides the diameter and its change over time, many other clinical risk factors have been proposed including

Figure 1. Clinically used criteria to assess abdominal aortic aneurysm rupture risk. Data were collected with an online survey of European vascular clinicians [32].

biomechanical risk indices [7-16], AAA shape [19, 20], female sex [7, 21-25], family susceptibility [25-27], high mean arterial pressure (MAP) [3], smoking and fluorodeoxyglucose (FDG) uptake on positron emission tomography (PET) [28, 29], a thick intraluminal thrombus (ILT) layer [18, 30], and rapid increase in ILT volume [31].

In summary, an AAA rupture is a complex event, and a better understanding requires a *multi-disciplinary* approach that is sensitive to *local* processes in the AAA wall.

The Biomechanical Rupture Risk Assessment (BRRA) method

AAA rupture is a *local* failure event in the wall that occurs when mechanical stress overcomes wall strength and naturally motivates tools of *local* wall rupture risk assessment. AAA wall pathology is driven by the complex interaction of biochemical and biomechanical events [33], such that a multidisciplinary approach is needed to better understand and more effectively treat AAA disease. Specifically, the Biomechanical Rupture Risk Assessment (BRRA) (usually based on finite element (FE) modeling) supports such a holistic risk assessment and quantitatively integrates many known AAA risk factors [7, 34]. Simply put, biomechanics investigates the stress and strain in biological tissue (basic BRRA-related terminology is listed in Table 1, and biomechanical indices like peak wall stress (PWS, see [35] and references therein) and the peak wall rupture index (PWRI) [13, 16, 36], have been regularly shown to be higher in ruptured/symptomatic AAAs than in intact/nonsymptomatic AAAs.
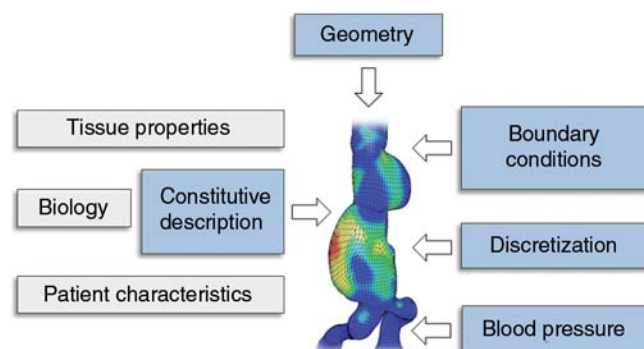
AAA Wall Stress: A Hypothetical Local Load Parameter Predicted by Structural Analysis Computations

AAA wall stress is the mechanical response to external forces (like blood pressure) acting on the vessel. Wall stress cannot be measured and is predicted (calculated) by solving the equilibrium equations under certain boundary and initial conditions. These equations can only be solved analytically (exactly) for a small number of rather simple problems. One of these simple solutions is the well-known *Laplace*

Table 1. Basic biomechanical definitions and terminology relating to the Biomechanical Rupture Risk Assessment of abdominal aortic aneurysm.

Stress	Stress is force normalized by the area through which it is transmitted.

Normal stress: Force acts normal to the area; $\sigma = \dfrac{N}{A}$, see Figure 2. Panel A.

Shear stress: Force acts in parallel to the area; $\tau = \dfrac{S}{A}$, Figure 2. Panel B.

The unit of the stress is Newton per square meter (N/m^2) or Pascal (Pa), which is the stress that arises if the force of one Newton is distributed over an area of one square meter.
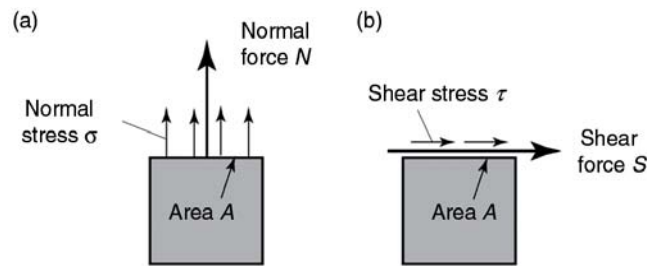
Figure 2. Definition of normal *Panel A*. and shear *Panel B*. stress.

A general three-dimensional state of stress is characterized by in total six independent stress components (i.e., three normal stresses and three shear stresses, respectively). Equivalent stresses like the von Mises equivalent stress σ_M, are used to express a multidimensional stress by a single stress value.

In vascular biology wall shear stress due to blood flow and wall normal stress due to blood pressure are prominent stresses. Wall shear stress from a steady flow q of viscous (Newtonian) fluid through a cylindrical tube of radius Y reads $\tau = \dfrac{4}{\pi r^3}\,q$, where μ denotes the dynamic viscosity. Circumferential wall stress σ_θ (normal stress along the circumferential direction) of a cylindrical tube that is pressurized by the inflation pressure p reads $\sigma_\theta = p\dfrac{d}{2h}$ where d and h denote the tube's diameter and wall thickness, respectively. In contrast axial wall stress σ_z (normal stress along the axial direction) of the pressurized cylindrical tube, which can freely deform in the axial direction, reads $\sigma_\theta = p\dfrac{d}{4h}$. For an AAA rupture risk assessment, circumferential σ_θ and σ_z axial stresses dominate the loading such that the vascular wall can be regarded at principal plane stress. Under this condition, the von Mises equivalent stress reads $\sigma_M = \sqrt{\sigma_\theta^2 - \sigma_\theta \sigma_z + \sigma_z^2}$.

Remark: Different stress definitions exist, and the Cauchy stress or true stress is most frequently used. Others stresses are Engineering stress, Second Piola–Kichhoff stress, etc., and the reader is referred to the finite strain continuum mechanics literature [37].

Tension	Tension in a membrane is defined as force normalized by length through which it is transmitted, see Figure 3. Consequently, the tension is independent from the thickness of the membrane. The unit of the tension is Newton per meter (N/m) or Pascal meter (Pa m), which is the tension that arises if the force of one Newton is distributed over a length of one meter.

(*table continues*)

Table 1. (*continued*)
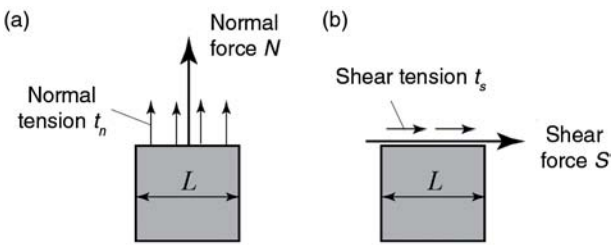
Tension (continued)	

Figure 3. Definition of normal *Panel A*. and shear *Panel B*. tension.

Strain

Strain is a dimensionless measure of deformation, and, similar to stress, both normal strain and shear strain can be defined, see Figure 4. Normal strain $\varepsilon = \frac{v}{L}$ reflects the change of length, while shear strain $\gamma = \frac{u}{L}$ reflects the change of angle. The strain is a dimensionless quantity.
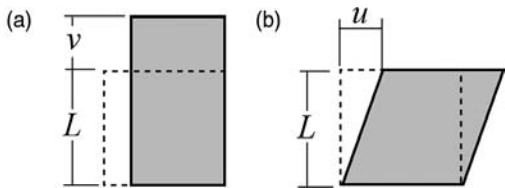

Figure 4. Definition of normal *Panel A*. and shear *Panel B*. strain. The dashed line denotes the originally undeformed body.

A general three-dimensional state of stain is characterized by in total six independent strain components (i.e., three normal strains and three shear strains, respectively). Vascular tissue can significantly deform and typically requires finite strain theory (i.e., the displacements u and v are in the same range as the dimension L), see Figure 4.

Constitutive model

A constitutive model is a mathematical description of the tissue's constitution. A sub-class of constitutive models relates stress and strain (i.e., specify how much stress develops at a certain state of strain and vice versa). Elastic models assume that the deformation energy (mechanical energy required to deform body) is fully recovered after unloading (i.e., dissipative effects are negligible). In contrast, viscoelastic models (a class of dissipative models) assume that the deformation energy is only partly transformed into tissue deformation, and some part of the energy is transformed into heat (i.e., cannot be recovered by unloading). Another class of constitutive models assumes the tissue being multiphasic. For example, a poroelasticity model regards an elastic solid (skeleton) phase immersed in a fluid phase to describe the constitution of the tissue.

Vascular tissue is nonlinear (i.e., it is soft at low strains and stiff at high strains, see Figure 5. For the passive vessel wall the soft (low strain) and stiff (high strain) responses are determined by elastin and collagen, respectively.

(*table continues*)

Table 1. (*continued*)

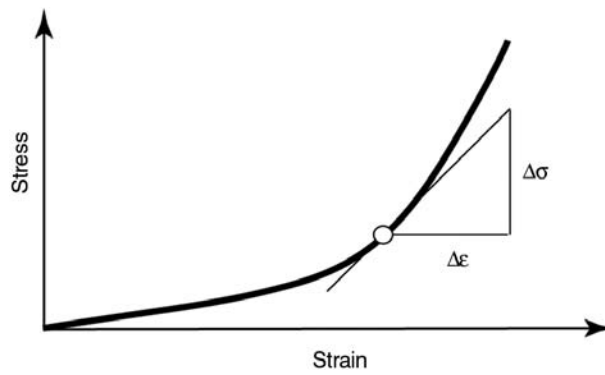|	
Constitutive model (continued)	

<div align="center">

Figure 5. Typical stress strain curve of vascular tissue. The stiffness at a certain strain is defined by the tangent to the stress strain curve.

</div>

Strength	Strength is the stress level at which failure appears. Depending how the tissue is loaded (i.e., how stress is applied), different types of strengths are defined. For example, the UTS is the stress level at which tissue fails at slowly increasing tensile stress.
	To characterize the strength under multiaxial stress conditions equivalent stresses like the von Mises equivalent stress σ_M are used, and the tissue is assumed to fail if σ_M reaches the tissue strength.
Tissue failure	Tissue failure is an event that causes mechanical or physiological changes, which in turn result in compromised tissue function. For the AAA rupture risk assessment, tissue failure is defined by the loss of its passive structural integrity.
Stiffness	The stiffness $k = \dfrac{\sigma}{\varepsilon}$ is a tissue-specific parameter that describes how stress increases at increasing strain (i.e., it is the tangent to the stress strain curve, see Figure 5). Vascular tissue is nonlinear, such that its stiffness is not constant but dependent on the strain state. Consequently, one and the same vessel will have different stiffness at different inflation pressures.
Anisotropy	Depending on the microstructural arrangement of cells and ECM vascular tissue shows macroscopic anisotropic properties (i.e., its mechanical properties depend on the direction along which they are evaluated). Consequently, tensile tests with wall strips along the circumferential and the axial vessel direction reveal different results.
Incompressibility	During physiological deformations, the volume of vascular tissue remains (almost) unchanged (i.e., the tissue is (almost) incompressible). This is mainly explained by the high content of not particularly mobile fluid within the tissue.
Equilibrium equations	At any time external forces, like blood pressure, that act on the vessel need to be balanced by internal tissue forces (i.e., by tissue stresses). These balance equations are called equilibrium equations, and specify a set of so-called partial differential equations that have to be satisfied locally (i.e., at each point in the tissue). In addition to the equilibrium equations, equations such as the conservation of mass for nongrowing tissue need to be satisfied. Finally, in order to complete the biomechanical description, boundary conditions and initial conditions specify how the vascular body interacts with its surrounding and denote its respective conditions at the beginning of the calculation. The whole set of equations can be solved by numerical methods like the FE method.

(*table continues*)

Table 1. (*continued*)

Length-scale	Like all other materials the vessel wall too is hierarchically built-up by different structural constituents that span length-scales ranging from the atomistic up to the macroscopic levels. The definition of stress and strain critically relies on the continuum assumption (i.e., the matter in the body is continuously distributed and fills the entire region of space it occupies). More specifically, the continuum assumption hinges on the concepts of an RVE. An RVE is a volume which includes a sufficiently large number of different structural constituents such that the RVE's mechanical response can be regarded as continuous. The size of the RVE defines the length-scale that relates to stress and strain.
FE Method	The FE method is a numerical concept for the approximate solution of many engineering problems (i.e., problems that are characterized by local equilibrium conditions under certain boundary conditions and initial conditions). In order to solve such problems with the FE method, the continuum is discretized (i.e., the vascular body is split into a large number of regular structural elements, the so-called FEs). The accuracy of the FE solution increases with the number of finite elements. Specifically, a certain number of elements is required to provide a sufficiently accurate solution (i.e., to keep the difference between the FE solution and the exact solution acceptably small). The difference between the FE solution and the exact solution is called discretization error.

AAA = abdominal aortic aneurysm; BRRA = biomechanical rupture risk assessment; ECM = extracellular matrix; FE = finite element; RVE = representative volume element; UTS = Ultimate Tensile Strength.

equation, which gives the wall stress for an inflated thin-walled circular tube, see Figure 6, Panel A. AAA geometry is complex and in most cases cannot be approximated by a thin-walled cylinder, such that wall stress predictions become much more challenging. Specifically, for these biomechanical problems the equilibrium equations can no longer be solved analytically, and wall stress predictions require approximate numerical approaches like the FE method, see Figure 6. Panel B. FE-based wall stress predictions require:

- Three-dimensional (3D) geometry of the ILT and the vessel wall.
- Mechanical characteristics (constitutive descriptions) of the ILT and wall tissue.
- Assumptions on how the AAA interacts with its surrounding.
- The blood pressure at which wall stress is predicted.

This input information is subjected to uncertainty, and its influence (sensitivity) on wall stress predictions needs to be carefully validated.

Uncertainty of Model Predictions

Naturally, every model involves making modeling assumptions (see Figure 7 for the BRRA) and reflects the real object only up to a certain degree of completeness (see A. Einstein: "Everything should be made as simple as possible, but no simpler." [38]), and a model should be verified and validated to the degree needed for the model's intended purpose or application [39]. For a BRRA simulation, the required level of modeling details can only be defined in the context of the clinical outcome. Consequently, a good model will only include modeling details that improve the clinical outcome and disregard all the other information that reflects our current knowledge about the biomechanical problem. For example, the required degree of complexity of the aneurysm wall model (isotropic vs. anisotropic modeling, single phase vs. multiphase modeling, constant wall thickness vs. variable wall thickness, etc.) used by the BRRA can only be evaluated in relation to the wall model's implication on the
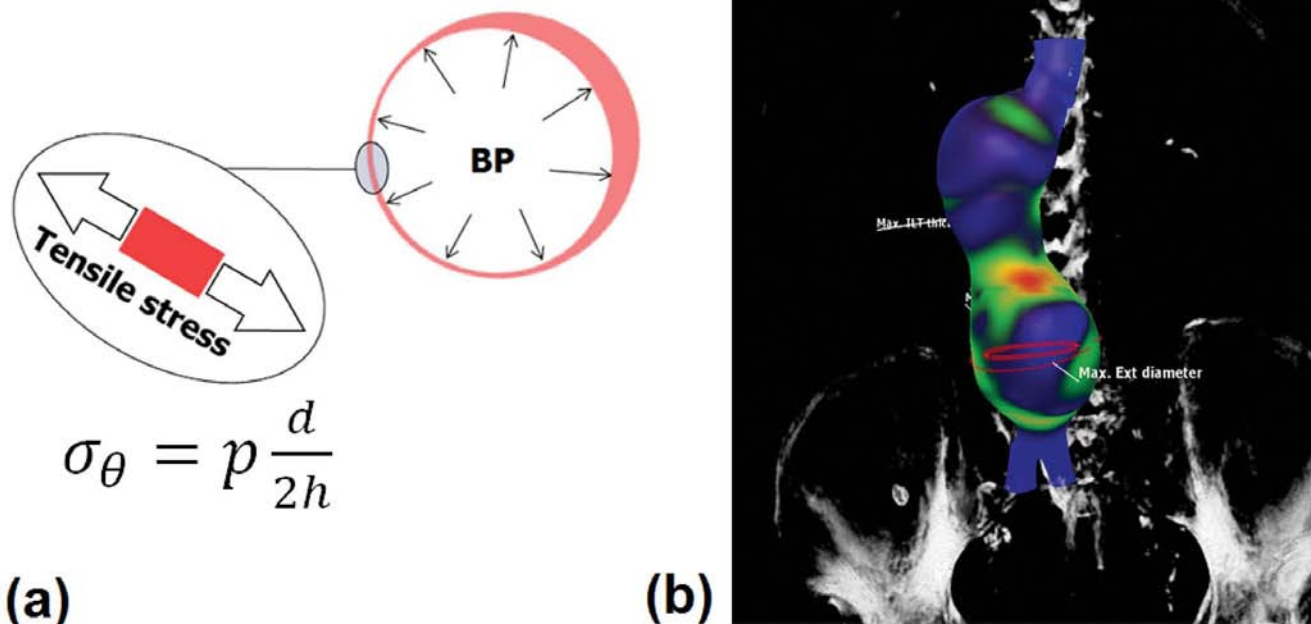
Figure 6. Wall stress predictions by solving the equilibrium equations. *Panel A*. Laplace equation gives the circumferential stress σ_θ of an inflated thin-walled cylindrical tube (pressure: p; diameter: d; wall thickness: h). *Panel B*. Distribution of the von Mises stress σ_M (red, high; blue, low) in the wall of an abdominal aortic aneurysm predicted by the finite element method.
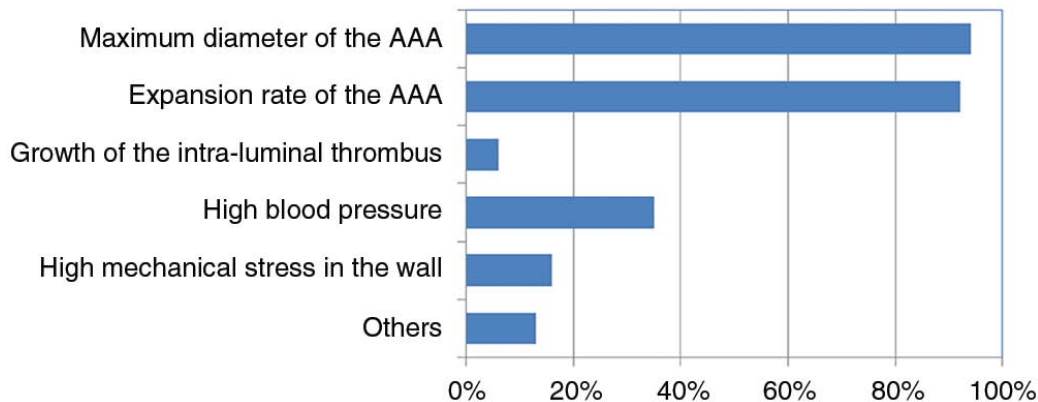
Figure 7. Modeling assumptions and input uncertainties entering the Biomechanical Rupture Risk Assessment (BRRA) of abdominal aortic aneurysms. The validity of each assumption needs to be validated with respect to the clinical outcome of the BRRA prediction. AAA = Abdominal aortic aneurysm.

clinical outcome – *a complex model does not necessarily give better diagnostic information*.

Wall stress computations are not particularly sensitive to constitutive descriptions as long as the wall's low initial stiffness, followed by its strong stiffening at higher strains (see Figure 5) is respected [40-42].

Similarly, despite the fact that ITL tissue is highly porous [43, 44], previous biomechanical studies have demonstrated that a single-phase model predicts AAA wall stress with sufficient accuracy [45, 46]. In contrast, wall stress predictions are sensitive to AAA geometry such that an accurate 3D AAA representation is criti-

cally important for accurate predictions. Finally, the FE method solves a discretized biomechanical model (i.e., the wall and ILT are represented by a large number of small regular structural elements, the so-called FEs). The discretization error becomes unacceptably large if the number of FEs used by the wall stress calculation is too small.

Macro Failure due to Accumulated Microstructural Tissue Damage

Mechanical force is transmitted from the macroscopic (tissue) scale down to the atomic scale, and different microstructural constituents are loaded differently. Consequently, increased blood pressure (macroscopic load) leads to local stress concentrations in the wall, and, if high enough, starts to damage the wall at specific spots. For example, microdefects like breakage and/or pullout of collagen fibrils gradually develop, weakening and softening the vessel wall. Because of the compromised biological integrity of aneurysm tissue and/or the supraphysiologic stress level, healing might not fully repair these microdefects. Consequently, the vessel wall continues to accumulate weak links, which in turn irreversibly diminish its strength. If the damage level (i.e., the numbers of defects per tissue volume) exceeds a certain threshold, microdefects join each other and form macrodefects. Finally, a single macrodefect may propagate and rupture the vessel through the whole thickness (i.e., the AAA ruptures). Different engineering concepts are known to study initiation and propagation of failure (macrodefects) in materials. One of the simplest approaches is introducing a risk factor by relating local wall stress and local wall strength termed the wall rupture index (WRI).

$$WRI = \frac{Wall\ stress}{Wall\ strength} \tag{1}$$

The WRI is a local parameter calculated all over the aneurysmal sack, and the BRRA therefore fully supports a local AAA risk assessment. Finally, the peak wall rupture index (PWRI) is the peak of the WRI is extracted all over the aneurysmal sack and serves as the final risk index of the BRRA.

Constitutive Modeling to Characterize Tissue Properties

The mechanical properties of vascular tissue are especially complex and are influenced by patient characteristics, disease progression, and local biological activity among other factors. Despite some methods suggesting in vivo tissue characterization, most current approaches apply in vitro (destructive) mechanical testing. In vitro mechanical testing allows for independent control of tissue strain and stress during testing (i.e., it supports tissue characterization at well-controlled loading conditions). Planar biaxial tensile testing is one frequently applied method for destructive AAA tissue characterization (see Figure 8, Panel A) and provides mean-population properties for the BRRA [47, 48]. It is frequently claimed that patient-specific elastic tissue properties might further improve the clinical value of the BRRA, although the current literature does not support this statement [42].

AAA Wall Thickness

The thickness of the AAA wall is nonuniform [49-51], influenced by many factors [52], and may [53] or may not [54] change between ruptured and
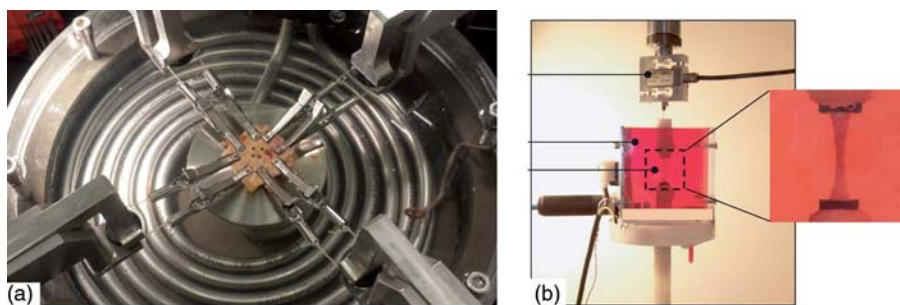

Figure 8. Mechanical characterization of aortic wall tissue. *Panel A*. Biaxial testing to identify elastic tissue properties. *Panel B*. Uniaxial testing of bone-shaped specimens to identify wall strength.

nonruptured AAAs. Wall thickness appears to play a dual role in the evaluation of aneurysm rupture risk. A thick AAA wall may suggest severe inflammation of the AAA tissue [17], indicating regions at higher risk of rupture, while thin-walled areas could be exposed to high wall stress and be at high risk for rupture. Biomechanical AAA studies report different average population thicknesses (see Table 2, which may be explained by fundamentally different measurement methods and the difficulty specifying the outer border of the adventitia.

AAA Tissue Elastic Properties

Due to the aneurysm-related proteolytic degeneration of structural proteins [83], an AAA wall

Table 2. Abdominal aortic aneurysm wall thickness and strength measured from In vitro tensile testing.

Reference	Sample definition	Wall thickness (mm)	Wall strength (MPa)
[1]	$n = 31$, fibrous	1.2	1.2
	$n = 38$, partly calcified	1.5	0.87
[48]	$n = 28$	1.18	-
[64]	$n = 83$	-	0.81
[47]	$n = 26$	1.32	-
[57]	$n = 25$, AAA diameter < 55 mm	1.53	0.77
	$n = 65$, AAA diameter > 55 mm	1.58	1.03
[58]	$n = 76$	-	Female: 0.68
			Male: 0.88
[17]	$n = 163$	1.57	1.42
[51]	$n = 374$ thickness, $n = 48$ tensile test	1.48	1.26
[65]	$n = 14$	1.5 to 1.9	Longitudinal: 0.93
			Circumferential: 1.15
[66]	$n = 16$	2.06	0.57
[59]	Anterior: $n = 29$	2.73	Longitudinal: 0.38
			Circumferential: 0.52
	Lateral: $n = 9$	2.52	Longitudinal: 0.51
			Circumferential: 0.73
	Posterior: $n = 9$	2.09	Longitudinal: 0.47
			Circumferential: 0.45
[53]	Intact AAA: $n = 26$	2.5	0.82
	Ruptured AAA: $n = 13$	3.6	0.54
[54]	Intact: $n = 278$ thickness, $n = 56$ tensile test	1.5	0.98
	Ruptured: $n = 141$ thickness, $n = 21$ tensile test	1.7	0.95
[60]	Longitudinal: $n = 45$	-	0.86
	Circumferential: $n = 19$	-	1.02
[18]	ILT layer thickness > 4 mm: $n = 7$	-	1.38
	ILT layer thickness < 4 mm: $n = 7$	-	2.16
Median (SD)		**1.58 (SD 0.64)**	**0.87 (SD 0.39)**

AAA = abdominal aortic aneurysm; ILT = intraluminal thrombus.

mechanically differs significantly from a normal aorta. Specifically, the AAA wall is less anisotropic, and, at the same time, the nonlinearity of the stress-strain relation is more pronounced [47]. Constitutive models for the AAA wall [40] and the ILT [61, 62] are mainly based on isotropic finite strain formulations with mean population parameters identified from in vitro tissue testing.

AAA Wall Strength

Wall strength cannot be estimated in vivo and always requires destructive (in vitro) testing. The multiaxial stress state at which vascular tissue is exposed in vivo can hardly be realized by in vitro experiments, such that wall strength information is usually derived from simplified sample loadings. With some very few exceptions [63], wall strength data have been collected from uniaxial tissue testing (i.e., tearing apart wall strip samples; see references in Table 2) as shown in Figure 8, Panel B.

As indicated by the AAA wall's inhomogeneous pathohistology [68], wall strength also shows significant inter- and intrapatient variability [17]. Strength values reported in the literature are summarized in Table 2. Despite the difference in strength values being largely caused by differences in wall thickness measurements, in vitro wall testing also identified several influential factors on wall strength (see Table 3). Most interestingly, some of these factors clearly conflict with the current clinical understanding of rupture risk.

For example, chronic obstructive pulmonary disease (COPD) increases wall strength (i.e., would be a negative risk factor), which has recently been supported by the fact that COPD patients' aneurysms rupture at larger diameters [67]. However, COPD is often regarded as an additional risk factor in the clinic.

Wall strength and thickness are inversely related leading to a strong negative correlation coefficient of –0.71 according to the data shown in Table 2 [17, 53, 54, 66, 69]. Consequently, local variations of wall thickness and wall strength partly compensate for each other [69], and wall tension (stress multiplied by wall thickness) seems to be a more robust rupture risk predictor [54]. The inverse correlation between wall thickness and wall strength also justifies, to some extent, the typically used uniform wall thickness for the BRRA computations. Consequently, FE models that assumed a homogeneous wall strength and wall thickness gave better results than models that used an inhomogeneous wall thickness and also regarded homogenous wall strength [69].

Work Flow

A robust, fast, and operator-insensitive simulation pipeline is required to implement the BRRA in the clinical work flow. As an example, Figure 9, Panel A illustrates the BRRA work flow using the A4clinics software (VASCOPS GmbH, Graz, Austria). During an *Image Segmentation* step, an accurate 3D model of the aneurysm is derived by segmenting
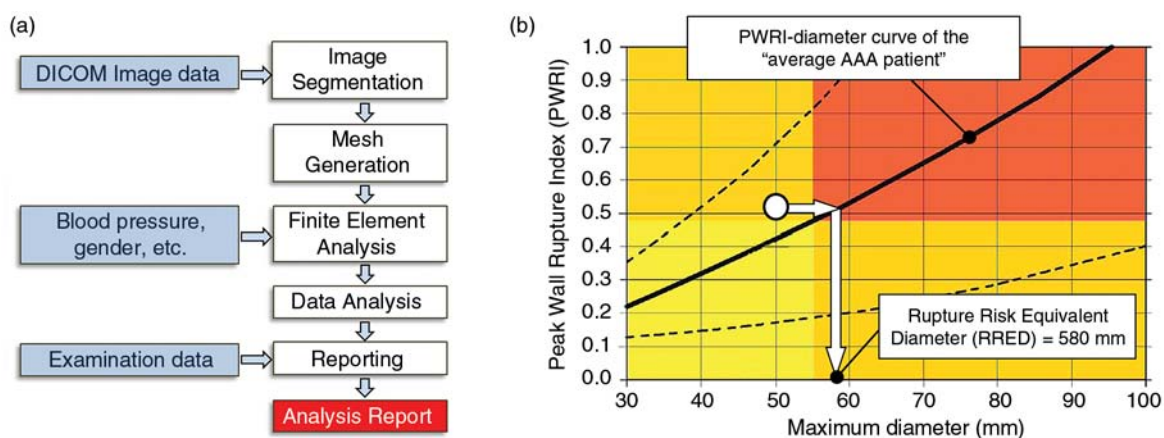

Figure 9. *Panel A*. Work flow of the Biomechanical Rupture Risk Assessment of abdominal aortic aneurysms (AAA) using A4clinics software (VASCOPS GmbH, Graz, Austria). *Panel B*. Definition of the Rupture Risk Equivalent Diameter (RRED) for an individual AAA patient. The RRED denotes the diameter of an average AAA that experiences the same peak wall rupture index as the individual case.

Table 3. Influential Factors on abdominal aortic aneurysm wall strength identified through in vitro tissue testing.

Factor	Influence on AAA wall strength	Reference(s)
Age	No	[17, 48, 53, 54, 64, 66]
Smoking	No	[17, 53, 54, 64]
Female sex	Decreasing	[58, 64]
	No	[17, 48, 52]
Presence of a thick ILT layer	Decreasing	[64, 69]
Large relative AAA size	Decreasing	[64]
	No	[17, 48, 53]
Ruptured AAAs in family history	Decreasing	[64]
COPD	Increasing	[66]
Anterior and posterior AAA wall surfaces	No	[54, 57]
Thick wall	Decreasing	[17, 52-54, 66]
Ruptured AAA when compared to nonruptured cases	Decreasing	[53]
	No	[17, 48, 52, 54, 57]
Hypoxia	Decreasing	[69]
Diabetes mellitus	Decreasing	[17, 52]
Potassium	Decreasing	[17]
Chronic kidney disease	Increasing	[52]
Hypercholesterolemia	Decreasing	[52]
Calcification	Decreasing	[52, 55, 56]
Angiotensin-converting-enzyme inhibitor	Decreasing	[52]
Maximum aneurysm diameter	Increasing	[57]
	No	[66]
Circumferential direction when compared to longitudinal direction	No	[57, 60, 65]
	Increasing	[59]

AAA = abdominal aortic aneurysm; COPD = chronic obstructive pulmonary disease; ILT = intraluminal thrombus.

luminal and exterior surfaces from computed tomography angiography (CT-A) images. A *Mesh Generation* step uses this information to mesh the wall and ILT (i.e., to split these volumes into a large number (~20,000-60,000) of FEs). A predefined wall thickness is used. During the *FE Analysis* step, the user sets the patient-individual MAP and other characteristics, and the FE method calculates the wall stress that is required to carry the blood pressure for the individual aneurysm shape and ILT topology. This calculation is based on mean population elastic tissue properties. Simultaneously, the wall stress is locally related to an estimated wall strength, which in turn defines the WRI over the entire aneurysmal sack. Finally, a *Data Analysis* step extracts key geometric and biomechanical informa-

tion, which together with other examination input is compiled by a *Reporting* step into an *Analysis Report*. All steps can be executed by clinical users, and the whole process from reading the Digital Imaging and Communications in Medicine (DICOM) images to receiving the *Analysis Report* takes about 10-20 minutes using standard laptops or PCs.

Definition of the Rupture Risk Equivalent Diameter (RRED)

To assess the relative risk of rupture with respect to the mean population AAA patient, the Rupture Risk Equivalent Diameter (RRED) is introduced, see Figure 9, Panel B. The RRED reflects the size of the average aneurysm that experiences the same PWRI as the individual case by translating the in-

dividual biomechanical analysis into a diameter risk (i.e., the most commonly applied risk stratification parameter) [16]. Consequently, the RRED connects the individual biomechanical assessment with the outcome of large diameter-based clinical trials, like the small United Kingdom aneurysm trial [1].

Validation of the BRRA

Prior to the implementation of the BRRA into the regular clinical workflow, its validity needs to be tested with respect to its specific simulation objective (i.e., the clinical value of the BRRA diagnosis) [39]. Specifically, it is not important that all underlying modeling assumptions (submodels) reflect current knowledge (see Section "*Uncertainty of Model Predictions*"), but the whole system needs to demonstrate an improvement over state-of-the-art clinical practice.

Operator Variability

Intra- and interoperator variability of the A4clinics (VASCOPS GmbH, Graz, Austria) rupture risk assessment system has been tested in clinical environments [70, 71], and the latest (as yet unpublished) data comes from James Cook University, Queensland, Australia, showing an intraoperator variability of 3.3% for PWRI

predictions and 1.6% for maximum diameter measurements. This high precision could only be achieved with active (deformable) image segmentation models known to have subpixel accuracy [1, 72]. In contrast other segmentation tools (e.g., MIMICS, Materialise, Leuven, Belgium) apply low-level segmentation methods based on threshold approaches, which require intensive manual interactions and leads to high operator variability of the results.

Retrospective Comparison between Ruptured and Nonruptured AAAs

The diagnostic value of the BRRA method has been studied for almost 20 years. Early work focused on PWS as a risk indicator (i.e., the effect of the inhomogeneous AAA wall strength was neglected in the assessment), and most studies disregarded the structural impact of the ILT on wall stress predictions. PWS has been regularly shown to be higher in ruptured/symptomatic AAAs than in intact/nonsymptomatic AAAs, see Figure 10, which was adapted from a recent meta-analysis [35].

Correlating mechanical in vitro tests with patient characteristics, defined a noninvasive, predictive model for the inhomogeneous strength of the AAA wall [64]. Consequently, local wall stress could be related to local wall strength, such that both key
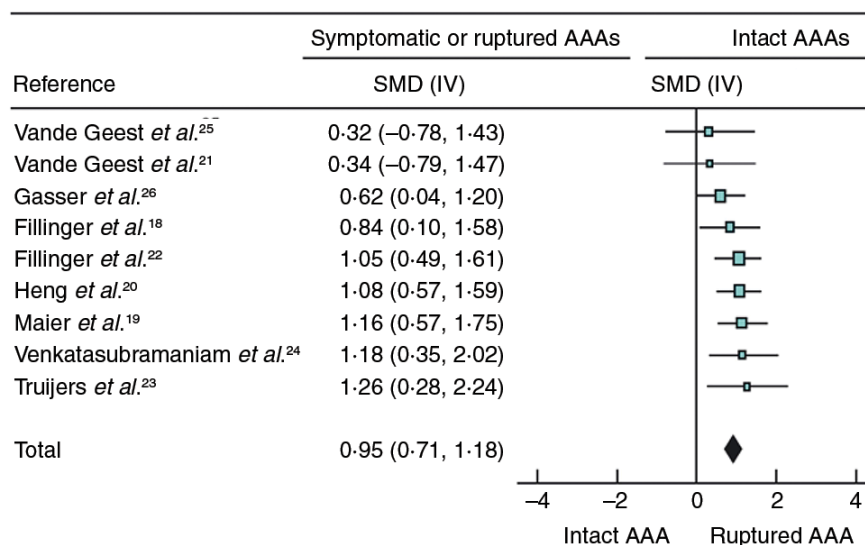
Reference	Symptomatic or ruptured AAAs SMD (IV)	Intact AAAs SMD (IV)
Vande Geest et al.[25]	0·32 (−0·78, 1·43)	
Vande Geest et al.[21]	0·34 (−0·79, 1·47)	
Gasser et al.[26]	0·62 (0·04, 1·20)	
Fillinger et al.[18]	0·84 (0·10, 1·58)	
Fillinger et al.[22]	1·05 (0·49, 1·61)	
Heng et al.[20]	1·08 (0·57, 1·59)	
Maier et al.[19]	1·16 (0·57, 1·75)	
Venkatasubramaniam et al.[24]	1·18 (0·35, 2·02)	
Truijers et al.[23]	1·26 (0·28, 2·24)	
Total	0·95 (0·71, 1·18)	

Figure 10. Diagnostic value of peak wall stress as risk indicator of the Biomechanical Rupture Risk Assessment of abdominal aortic aneurysms (AAA). Data are based on the retrospective comparison between ruptured/symptomatic AAAs and intact/nonsymptomatic AAAs. Adapted from Khosla et al. [35].

factors of the BRRA were addressed. Integrating wall strength in the BRRA further improved its diagnostic value (i.e., led to an improved retrospective discrimination between ruptured and nonruptured cases). For example, a size-adjusted comparison showed that the RRED was, on average, 14.0 mm larger in ruptured than in nonruptured cases ($p < 0.001$), see Figure 11 taken from [16]. Similar results have been presented elsewhere [13]. These findings have recently been confirmed by the clinical observation that a high PWRI value in nonsymptomatic AAA patients seems to be a negative prognostic factor [73].

Quasiprospective Comparison between Ruptured and Nonruptured AAAs

CT-A scans of AAA patients that eventually experienced rupture (e.g., because the patient refused treatment) provide ideal data for a quasiprospective validation of the BRRA, and, to the best knowledge of the author, only one such study has been published [74]. The results showed that the BRRA method was able to significantly discriminate between AAAs that would rupture compared to a baseline-matched control group that did not rupture or was treated. The study also found that in more than half of the cases, the rupture sites correlated with calculated prerupture PWRR locations. Consequently, the authors concluded that asymptomatic AAA patients with high

PWRR and RRED values have an increased rupture risk.

Correlation between PWRI and the Annual AAA Rupture Risk

Plotting the PWRI as a function of the diameter allows relating it to the annual AAA rupture risk from observational studies [16]. Figure 12 shows such a plot, where the thick and thin lines denote PWRI and a summary of annual AAA rupture risk data, respectively [75]. The graph clearly demonstrates a progressive increase of PWRI with the diameter, which nicely reflects the clinically reported prevalence for AAA ruptures with increasing diameter. In addition, this plot allows direct translation of the PWRI into the annual risk for AAA rupture. For example, a PWRI of 0.56 corresponds to the annual risk of rupture of 16%, see Figure 12.

Female versus Male AAA Rupture Risk

Despite the fact that AAA prevalence is several times lower in females, female aneurysms rupture at smaller diameters [21, 22, 24]. Independently from this clinical observation, in vitro failure testing of female AAA wall samples showed a lower strength compared to male samples [58, 64]. This sex-specific wall weakening effect is integrated into the PWRI, and the biomechanical risk of an average 53-mm large female AAA relates to an average 13.2-mm
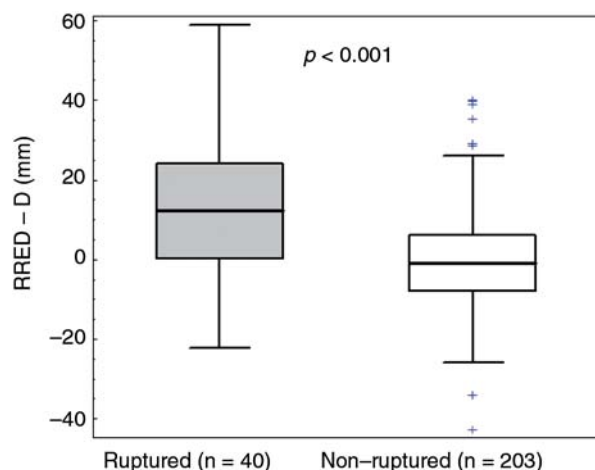

Figure 11. Retrospective and size-adjusted comparison between ruptured and nonruptured abdominal aortic aneurysms. The comparison is based on the difference between Rupture Risk Equivalent Diameter and the maximum transversal diameter (D). Adapted from Gasser et al. [16].
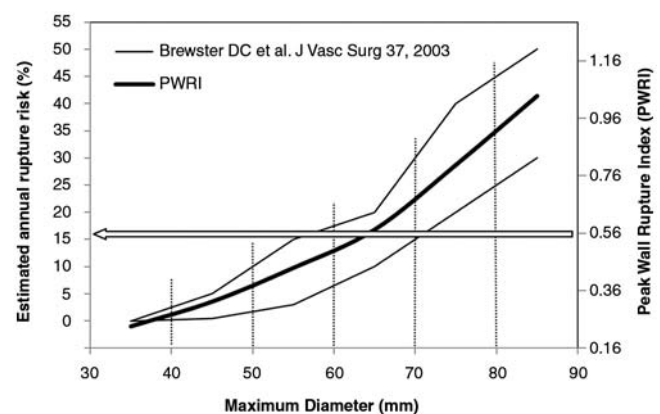

Figure 12. Relation between peak wall rupture index, annual risk of abdominal aortic aneurysm rupture (AAA), and its maximum diameter. Prediction with the Biomechanical Rupture Risk Assessment (thick line). Data from clinical observations of ruptured AAAs summarized in 75 (thin lines). Adapted from Gasser et al. [16].

larger male case (p = 0.014) [16]. This BRRA simulation result nicely matches data from clinical observation [21].

Correlation between PWRI and FDG Uptake

Vascular wall biological activity can be indirectly evaluated through energy consumption using 18-fluorodeoxyglucose (18F-FDG) as a tracer for positron emission tomography (PET) imaging [28, 75]. In addition vascular cells respond to mechanical loads such that an 18F-FDG-uptake can in principle be used to qualitatively explore mechanical aorta loading [33]. Despite the fact that the aneurysmal wall loses its biological vitality, PET images still showed a considerable correlation between wall stress and 18F-FDG uptake [29, 76].

Correlation between PWRI and Wall Histopathology

Biomechanical stress is a common denominator of several aortic pathologies [33]. The complex geometry and morphology of AAAs cause highly inhomogeneous wall stress and WRI distributions (see Figure 6, Panel B), which were found to correlate with wall histopathology. Specifically, wall segments that in vivo experienced high WRI showed fewer smooth muscle cells and elastic fibers, more soft and hard plaques, as well as a trend to more fibrosis compared to wall samples at low WRI [68].

Integration of AAA Growth Aspects

The above outlined method aims at assessing AAA rupture risk at a single time point, and, simply put, can be regarded as a "refined diameter criterion" (see Figure 14, Panel A) that accounts for the individual AAA morphology, blood pressure and other patient characteristics. However, such an approach is entirely static and completely neglects AAA growth (dynamics) aspects. The BRRA method is a generic, biomechanics-based approach, which provides interfaces to incorporate information from different research disciplines. As an example, in this section a possible approach to integrate AAA growth effects in the BRRA method is outlined that could (potentially) further improve BRRA sensitivity and specificity.

Aneurysm Growth

AAA growth is complex and distributed across the aneurysmal sack [6], and the significant variation in aneurysm expansion remains unexplained by global parameters like the maximum diameter alone [78], smoking [79], sex, and inflammation [80]. In addition to these effects, the local cross-section diameter, local ILT thickness, and local wall stress (among others) also influence AAA growth [81]. Most interestingly, wall stress only seems to
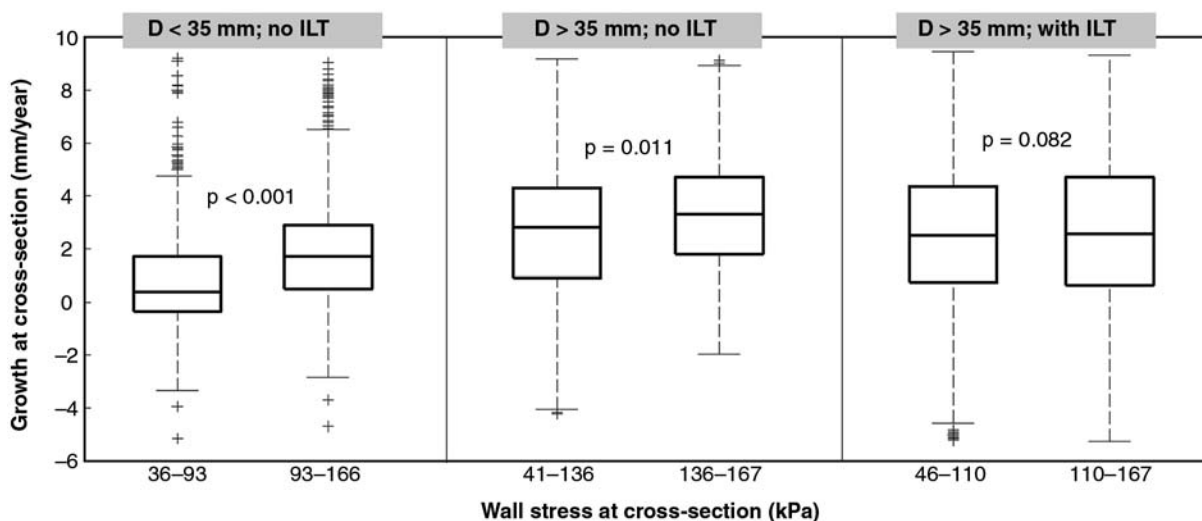

Figure 13. Effect of wall stress on abdominal aortic aneurysms cross-section growth. Cross-sections were taken perpendicular to the lumen center line, and the diameter D denotes their size. Small (nonaneurysmal) cross-sections free of intraluminal thrombus (ILT) (left). Large aneurysmal cross-sections free of ILT (middle). Large aneurysmal cross-sections covered by ILT (right). Sex, smoking status, and statin consumption were similar in all tested groups.
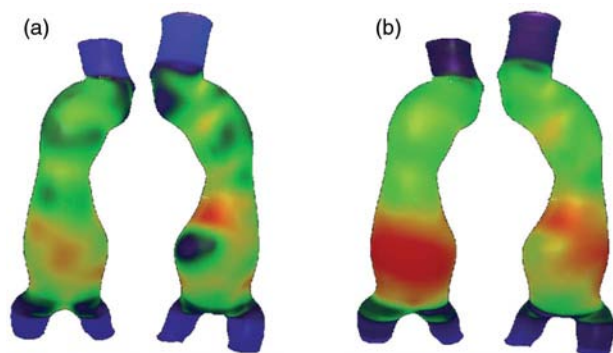
Figure 14. Color-coded risk index distributions over the aneurysmal sack of an individual abdominal aortic aneurysm. Red and blue indicate high and low risk, respectively. *Panel A*. Static risk expressed by the wall rupture index. *Panel B*. Dynamic risk expressed by a multiparametric growth model.

influence the growth rate of smaller AAA cross-sections and most dominantly cross-sections that are not covered by ILT (i.e., rather normal vascular wall sections, see Figure 13).

Fast Local Wall Growth Might Compromise Wall Strength

Collagen fibers in the vascular wall have a major impact on the mechanical properties at higher loads (i.e., at the condition experienced by the aneurysm wall) [82, 83]. Specifically, it seems that collagen is the only remaining histologic structure able to carry the high mechanical load of later-stage aneurysms [84, 85]. Collagen is under continuous turnover and the maintenance of the collagen network relies on a delicate balance between synthesis by fibroblasts and degradation by metalloproteinases. A malfunction of collagen turnover could fail to result in homeostasis and determine AAA disease (i.e., collagen synthesis is insufficient to counteract the increasing mechanical stress), such that aneurysm growth further accelerates [83].

Integration of Local Growth in the BRRA

It is likely that insufficient collagen remodeling diminishes local wall strength, which in turn increases the WRI. Consequently, integrating growth-related wall strength diminishing effects into the BRRA method could further improve its diagnostic value. Alternatively, local AAA wall growth that is predicted by a multiparametric AAA growth model could directly

serve as an additional risk index similar to a "refined growth criterion," see Figure 14, Panel B. Such a risk index reflects growth all over the aneurysmal sack and does not only inform how fast the maximum diameter expands. To date, a quantitative relation between local growth rate and local wall strength-diminishing effects is not available; further experimental data would be needed to establish such a relationship.

Conclusion

AAA rupture is a *local* event in the aneurysm wall that naturally requires tools for a *local* wall rupture risk assessment. Global parameters like the maximum diameter and its expansion over time can only provide very rough risk indications and frequently fail to predict individual risk for AAA rupture. In contrast, the BRRA method allows analyzing the wall's *local* mechanical loading (i.e., its risk of *local* rupture). To this end, the BRRA *quantitatively* integrates many known risk factors for AAA rupture like large size, asymmetric shape, female sex, and hypoxia due to a thick ILT layer and therefore supports a highly individualized risk assessment. The static biomechanical risk for rupture is best expressed by the RRED, which relates the individual case to the size of an average aneurysm at the same biomechanical risk for rupture. A significant and still growing body of validation evidence suggests using the RRED as an additional parameter for AAA repair indication. However, prospective experiences with the BRRA method are still missing.

More Complexity Does Not Necessarily Give Better Predictions

Many biomechanical models are overloaded with mechanical complexities and fail to address clinical problems adequately; therefore, they do not enjoy clinician acceptance. A simulation model represents the real objective or process towards the desired degree of complexity and should be guided by clinical needs rather than by integrating all available (biomechanical) information of the problem [39, 86]. Computational biomechanical models require careful selection and combination of modeling assumptions as well as rigorous clinical validation. Where would further improvement be most effective? Apart from

other challenges, biomechanical predictions critically depend on an accurate constitutive description of the AAA tissue. Most important for the BRRA is to estimate AAA wall strength, which by itself is influenced by many factors, see Table 3.

It is crucial in the development of a constitutive model to understand both the (passive) interaction of structural components within the vascular wall and how cells dynamically maintain such a structure. Vascular tissue senses and responds actively to changes in its mechanical environment, a crucial tissue property that is currently largely overlooked in the BRRA. However, modern image modalities allow the extraction of biomechanical functional information (gated CT-A, 3D ultrasound, MRI), as well as biological activity (PET scan) of the wall, which in turn could be directly put into the BRRA. Such information might provide valuable insights into growth-related wall strength diminishing effects, which in turn could further improve the sensitivity and specificity of the BRRA. Most important, the BRRA is a generic, biomechanics-based approach that provides several interfaces to couple it to other research disciplines such as biochemistry and genetics and fully supports a holistic understanding of AAA disease.

Acknowledgment

Conflict of Interest

The author is co-founder and shareholder of VASCOPS GmbH, Graz, Austria.

> **Comment on this Article or Ask a Question**

References

1. The UK Small Aneurysm Trial Participants. Mortality results for randomised controlled trial of early elective surgery or ultrasonographic surveillance for small abdominal aortic aneurysms. Lancet. 1998;352: 1649-1655. DOI: 10.1016/S0140-6736(98)10137-X

2. Greenhalgh RM, Powell JT. Endovascular repair of abdominal aortic aneurysm. N Engl J Med. 2008;358:494-501. DOI: 10.1056/NEJMct0707524

3. Brown LC, Powell JT. Risk factors for aneurysm rupture in patients kept under ultrasound surveillance. UK Small Aneurysm Trial Participants. Ann Surg. 1999; 230:289-296. DOI: 10.1097/00000658-199909000-00002

4. Nicholls SC, Gardner JB, Meissner MH, Johansen HK. Rupture in small abdominal aortic aneurysms. J Vasc Surg. 1998;28:884-888. DOI: 10.1016/S0741-5214(98)70065-5

5. Darling RC, Messina CR, Brewster DC, Ottinger LW. Autopsy study of unoperated abdominal aortic aneurysms. Circulation. 1977; 56:II161-II164. PMID: 884821

6. Martufi G, Auer M, Roy J, Swedenborg J, Sakalihasan N, Panuccio G, et al. Multidimensional growth measurements abdominal aortic aneurysms. J Vasc Surg. 2013;58:748-755. DOI: 10.1016/j.jvs.2012.11.070

7. Fillinger MF, Raghavan ML, Marra SP, Cronenwett JL, Kennedy FE. In vivo analysis of mechanical wall stress and abdominal aortic aneurysm rupture risk. J Vasc Surg. 2002; 36:589-597. DOI: 10.1067/mva.2002.125478

8. Fillinger MF, Marra SP, Raghavan ML, Kennedy FE. Prediction of rupture risk in abdominal aortic aneurysm during observation: wall stress versus diameter. J Vasc Surg. 2003; 37:724-732. DOI: 10.1067/mva.2003.213

9. Venkatasubramaniam AK, Fagan MJ, Mehta T, Mylankal KJ, Ray B, Kuhan G, et al. A comparative study of aortic wall stress using finite element analysis for ruptured and non-ruptured abdominal aortic aneurysms. Eur J Vasc Endovasc Surg. 2004;28:168-176. DOI: 10.1016/s1078-5884(04)00178-9

10. Vande Geest JP, Di Martino ES, Bohra A, Mackaroun MS, Vorp DA. A biomechanics-based rupture potential index for abdominal aortic aneurysm risk assessment: demonstrative application. Ann N Y Acad Sci. 2006;1085:11-21. DOI: 10.1196/annals.1383.046

11. Truijers M, Pol JA, Schultzekool LJ, van Strekenburg SM, Fillinger MF, Blankensteijn JD. Wall stress analysis in small asymptomatic, symptomatic and ruptured abdominal aortic aneurysms. Eur J Vasc Endovasc Surg. 2007;33:401-407. DOI: 10.1016/j.ejvs.2006.10.009

12. Vande Geest JP, Schmidt DE, Sacks MS, Vorp DA. The effects of anisotropy on the stress analyses of patient-specific abdominal aortic aneurysms. Ann Biomed Eng. 2008;36:921-932. DOI: 10.1007/s10439-008-9490-3

13. Maier A, Gee MW, Reeps C, Pongratz J, Eckstein HH, Wall WA. A comparison of diameter, wall stress, and rupture potential index for abdominal aortic aneurysm rupture risk prediction. Ann Biomed Eng. 2010;38:3124-3134. DOI: 10.1007/s10439-010-0067-6

14. Gasser TC, Auer M, Labruto F, Swedenborg J, Roy J. Biomechanical rupture risk assessment of abdominal aortic aneurysms: Model complexity versus predictability of finite element simulations. Eur J Vasc Endovasc Surg. 2010;40:176-185. DOI: 10.1016/j.ejvs.2010.04.003

15. McGloughlin TM, Doyle BJ. New approaches to abdominal aortic aneurysm rupture risk assessment: engineering insights with clinical gain. Arterioscler Thromb Vasc Biol. 2010; 30:1687-1694. DOI: 10.1161/ATVBAHA.110.204529

16. Gasser TC, Nchimi A, Swedenborg J, Roy J, Sakalihasan N, Böckler D, et al. A novel strategy to translate the biomechanical

rupture risk of abdominal aortic aneurysms to their equivalent diameter risk: Method and retrospective validation. Eur J Vasc Endovasc Surg. 2014;47:288-295. DOI: 10.1016/j.ejvs.2013.12.018

17. Reeps C, Maier A, Pelisek J, Härtl F, Grabher-Maier V, Wall WA, et al. Measuring and modeling patient-specific distributions of material properties in abdominal aortic wall. Biomech Model Mechanobiol. 2013;12:717-733. DOI: 10.1007/s10237-012-0436-1

18. Vorp DA, Lee PC, Wang DH, Makaroun MS, Nemoto EM, Ogawa S, et al. Association of intraluminal thrombus in abdominal aortic aneurysm with local hypoxia and wall weakening. J Vasc Surg. 2001;34:291-299. DOI: 10.1067/mva.2001.114813

19. Vorp DA, Raghavan ML, Webster MW. Mechanical wall stress in abdominal aortic aneurysm: influence of diameter and asymmetry. J Vasc Surg. 1998;27:632-639. DOI: 10.1016/S0741-5214(98)70227-7

20. Hua J, Mower WR. Simple geometric characteristics fail to reliably predict abdominal aortic aneurysm wall stresses. J Vasc Surg. 2001;34:308-315. DOI: 10.1067/mva.2001.114815

21. Heikkinen M, Salenius J, Zeitlin R, Saarinen J, Suominen V, Metsänoja R, et al. The fate of AAA patients referred electively to vascular surgical unit. Scand J Surg. 2002;91:345-352. PMID: 12558084

22. Brown PM, Zelt DT, Sobolev B. The risk of rupture in untreated aneurysms: the impact of size, gender, and expansion rate. J Vasc Surg. 2003;37:280-284. DOI: 10.1067/mva.2003.119

23. Wilson KA, Lee AJ, Hoskins PR, Fowkes FG, Ruckley CV, Bradbury AW. The relationship between aortic wall distensibility and rupture of infrarenal abdominal aortic aneurysm. J Vasc Surg. 2003;37:112-117. DOI: 10.1067/mva.2003.40

24. Derubertis BG, Trocciola SM, Ryer EJ, Pieracci FM, McKinsey JF, Faries PL, et al. Abdominal aortic aneurysm in women: prevalence, risk factors, and implications for screening. J Vasc Surg. 2007;46:630-635. DOI: 10.1016/j.jvs.2007.06.024

25. Darling RC 3rd, Brewster DC, Darling RC, LaMuraglia GM, Moncure AC, Cambria RP, et al. Are familial abdominal aortic aneurysms different? J Vasc Surg. 1989;10:39-43. DOI: 10.1016/0741-5214(89)90283-8

26. Verloes A, Sakalihasan N, Koulischer L, Limet R. Aneurysms of the abdominal aorta: familial and genetic aspects in three hundred thirteen pedigrees. J Vasc Surg. 1995; 21:646-655. DOI: 10.1016/S0741-5214(95)70196-6

27. Larsson E, Granath F, Swedenborg J, Hultgren R. A population-based case-control study of the familial risk of abdominal aortic aneurysm. J Vasc Surg. 2009;49:47-50. DOI: 10.1016/j.jvs.2008.08.012

28. Sakalihasan N, Van Damme H, Gomez P, Rigo P, Lapiere CM, Nusgens B, et al. Positron emission tomography (PET) evaluation of abdominal aortic aneurysm (AAA). Eur J Vasc Endovasc Surg. 2002;23:431-436. DOI: 10.1053/ejvs.2002.1646

29. Nchimi A, Cheramy-Bien JP, Gasser TC, Namur G, Gomez P, Seidel L, et al. Multifactorial relationship between 18F-fluoro-deoxy-glucose positron emission tomography signaling and biomechanical properties in unruptured aortic aneurysms. Circ Cardiovasc Imaging. 2014;7:82-91. DOI: 10.1161/CIRCIMAGING.112.000415

30. Kazi M, Thyberg J, Religa P, Roy J, Eriksson P, Hedin U, et al. Influence of intraluminal thrombus on structural and cellular composition of abdominal aortic aneurysm wall. J Vasc Surg. 2003;38:1283-1292. DOI: 10.1016/S0741-5214(03)00791-2

31. Stenbaek J, Kalin B, Swedenborg J. Growth of thrombus may be a better predictor of rupture than diameter in patients with abdominal aortic aneurysms. Eur J Vasc Endovasc Surg. 2000;20:466-499. DOI: 10.1053/ejvs.2000.1217

32. VASCOPS GmbH. On-line survey: Clinical assessment of AAA rupture risk. Are biomechanical predictors needed, 2006. Available at http://www.vascops.com/files/survey2006.pdf.

33. Bäck M, Gasser TC, Michel JB, Caligiuri G. Biomechanical factors in the biology of aortic wall and aortic valve diseases. Cardiovasc Res. 2013;99:232-241. DOI: 10.1093/cvr/cvt040

34. Vorp DA. Biomechanics of abdominal aortic aneurysm. J Biomech. 2007;40:1887-1902. DOI: 10.1016/j.jbiomech.2006.09.003

35. Khosla S, Morris DR, Moxon JV, Walker PJ, Gasser TC, Golledge J. Meta-analysis of peak wall stress in ruptured, symptomatic and intact abdominal aortic aneurysms. Brit J Surg. 2014;101:1350-1357 DOI: 10.1002/bjs.9578

36. Erhart P, Hyhlik-Dürr A, Geisbüsch P, Kotelis D, Müller-Eschner M, Gasser TC, et al. Finite element analysis in asymptomatic, symptomatic and ruptured abdominal aortic aneurysms – in search of new rupture risk predictors. Eur J Vasc Endovasc Surg. 2015;49:239-245. DOI: 10.1016/j.ejvs.2014.11.010

37. Bonet J, Wood RD. Nonlinear Continuum Mechanics for Finite Element Analysis. Cambridge University Press, Mar 13, 2008.

38. Quote investigator: Exploring the Origins of Quotes. Available at http://quoteinvestigator.com/2011/05/13/einstein-simple/#more-2363.

39. Sargent RG. Verification and validation of simulation models. Proceedings of the 2011 Winter Simulation Conference. http://www.informs-sim.org/wsc11papers/016.pdf

40. Raghavan ML, Vorp DA. Toward a biomechanical tool to evaluate rupture potential of abdominal aortic aneurysm: identification of a finite strain constitutive model and evaluation of its applicability. J Biomech. 2000;33:475-482. DOI: 10.1016/S0021-9290(99)00201-8

41. Di Martino ES, Vorp DA. Effect of variation in intraluminal thrombus constitutive properties on abdominal aortic aneurysm wall stress. Ann Biomed Eng. 2003;31:804-809. DOI: 10.1114/1.1581880

42. Polzer S, Gasser TC, Bursa J, Staffa R, Vlachovsky R, Man V, et al. Importance of material model in wall stress prediction in abdominal aortic aneurysms. Med Eng Phys. 2013;35:1282-1289. DOI: 10.1016/j.medengphy.2013.01.008

43. Adolph R, Vorp DA, Steed DL, Webster MW, Kameneva MV, Watkins SC. Cellular content and permeability of intraluminal thrombus in abdominal aortic aneurysm. J Vasc Surg. 1997;25:916-926. DOI: 10.1016/S0741-5214(97)70223-4

44. Gasser TC, Martufi G, Auer M, Folkesson M, Swedenborg, J. Micromechanical characterization of intra-luminal thrombus tissue from abdominal aortic aneurysms. Ann Biomed Eng. 2010;38:371-379. DOI: 10.1007/s10439-009-9837-4

45. Ayyalasomayajula A, Vande Geest JP, Simon BR. Porohyperelastic finite element modeling of abdominal aortic aneurysms. J Biomech Eng. 2010;132:104502. DOI: 10.1115/1.4002370

46. Polzer S, Gasser TC, Markert B, Bursa J, Skacel P. Impact of poroelasticity of intraluminal thrombus on wall stress of abdominal aortic aneurysms. Biomed Eng Online. 2012;11:62. DOI: 10.1186/1475-925X-11-62

47. Vande Geest JP, Sacks MS, Vorp DA. The effects of aneurysm on the biaxial mechanical behavior of human abdominal aorta. J Biomech. 2006;39:1324-1334. DOI: 10.1016/j.jbiomech.2005.03.003

48. O'Leary SA, Healy D, Kavanagh EG, Walsh MT, McGloughlin TM, Doyle BJ. The biaxial biomechanical behavior of abdominal aortic aneurysm tissue. Ann Biomed Eng. 2014;42:2440-2450. DOI: 10.1007/s10439-014-1106-5

49. Martufi G, Di Martino ES, Amon CH, Muluk SC, Finol EA. Three-dimensional geometrical characterization of abdominal aortic aneurysms: image-based wall thickness distribution. J Biomech Eng. 2009;131:061015. DOI: 10.1115/ 1.3127256.

50. Shum J, DiMartino ES, Goldhammer A, Goldman DH, Acker LC, Patel G, et al. Semi-automatic vessel wall detection and quantification of wall thickness in CT images of human abdominal aortic aneurysms. Med Phys. 2010;37:638-648. DOI: 10.1118/1.3284976

51. Raghavan ML, Kratzberg J, Castro de Tolosa EM, Hanaoka MM, Walker P, da Silva ES. Regional distribution of wall thickness and failure properties of human abdominal aortic aneurysm. J Biomech. 2006;39:3010-3016. DOI: 10.1016/j.jbiomech.2005.10.021

52. Maier A. Computational Modeling of Rupture Risk in Abdominal Aortic Aneurysms. Munich: Verlag Dr. Hut; 2013.

53. Di Martino ES, Bohra A, Vande Geest JP, Gupta N, Makaroun M, Vorp DA. Biomechanical properties of ruptured versus electively repaired abdominal aortic aneurysm wall tissue. J Vasc Surg. 2006;43:570-576. DOI: 10.1016/j.jvs.2005.10.072

54. Raghavan ML, Hanaoka MM, Kratzberg JA, de Lourdes Higuchi M, da Silva ES. Biomechanical failure properties and microstructural content of ruptured and unruptured abdominal aortic aneurysms. J Biomech. 2011;44:2501-2507. DOI: 10.1016/j.jbiomech.2011.06.004

55. Maier A, Gee MW, Reeps C, Eckstein HH, Wall WA. Impact of calcifications on patient-specific wall stress analysis of abdominal aortic aneurysms. Biomech Model Mechanobiol. 2010;9:511-521. DOI: 10.1007/s10237-010-0191-0

56. O'Leary SA, Mulvihill JJ, Barrett HE, Kavanagh EG, Walsh MT, McGloughlin TM, et al. Determining the influence of calcification on the failure properties of abdominal aortic aneurysm (AAA) tissue. J Mech Behav Biomed Mater. 2015;42:154-167. DOI: 10.1016/j.jmbbm.2014.11.005

57. Tavares Monteiro JA, da Silva ES, Raghavan ML, Puech-Leão P, de Lourdes Higuchi M, Otoch JP. Histologic, histochemical, and biomechanical properties of fragments isolated from the anterior wall of abdominal aortic aneurysms. J Vasc Surg. 2014;59:1393-1401. DOI: 10.1016/j.jvs.2013.04.064

58. Vande Geest JP, Dillavou ED, Di Martino ES, Oberdier M, Bohra A, Makaroun MS, et al. Gender-related differences in the tensile strength of abdominal aortic aneurysm. Ann N Y Acad Sci. 2006;1085:400-402. DOI: 10.1196/annals.1383.048

59. Thubrikar MJ, Labrosse M, Robicsek F, Al-Soudi J, Fowler B. Mechanical properties of abdominal aortic aneurysm wall. J Med Eng Technol. 2001;25:133-142. DOI: 10.1080/03091900110057806

60. Raghavan ML, Webster MW, Vorp DA. Ex vivo biomechanical behavior of abdominal aortic aneurysm: assessment using a new mathematical model. Ann Biomed Eng. 1996;24:573-582. DOI: 10.1007/BF02684226

61. Vande Geest JP, Sacks MS, Vorp DA. A planar biaxial constitutive relation for the luminal layer of intra-luminal thrombus in abdominal aortic aneurysms. J Biomech. 2006;39:2347-2354. DOI: 10.1016/j.jbiomech.2006.05.011

62. Gasser TC, Görgülü G, Folkesson M, Swedenborg J. Failure properties of intra-luminal thrombus in abdominal aortic aneurysm under static and pulsating mechanical loads. J Vasc Surg. 2008;48:179-188. DOI: 10.1016/j.jvs.2008.01.036

63. Romo A, Badel P, Duprey A, Favre JP, Avril S. In vitro analysis of localized aneurysm rupture. J Biomech. 2014;47:607-616. DOI: 10.1016/j.jbiomech.2013.12.012

64. Vande Geest JP, Wang DH, Wisniewski SR, Makaroun MS, Vorp DA. Towards a noninvasive method for determination of patient-specific wall strength distribution in abdominal aortic aneurysms. Ann Biomed Eng. 2006;34:1098-1106. DOI: 10.1007/s10439-006-9132-6

65. Xiong J, Wang SM, Zhou W, Wu JG. Measurement and analysis of ultimate mechanical properties, stress-strain curve fit, and elastic modulus formula of human abdominal aortic aneurysm and nonaneurysmal abdominal aorta. J Vasc Surg. 2008;48:189-195. DOI: 10.1016/j.jvs.2007.12.053

66. Forsell, C, Swedenborg J, Roy J, Gasser TC. The quasi-static failure properties of the abdominal aortic aneurysm wall estimated by a mixed experimental-numerical approach. Ann Biomed Eng. 2013;41:1554-1566. DOI: 10.1007/s10439-012-0711-4

67. Kubíček L, Staffa R, Vlachovský R, Polzer S, Kružliak P. Incidence of small abdominal aortic aneurysms rupture, impact of comorbidities and our experience with rup-

ture risk prediction based on wall stress assessment. Cor et Vasa. 2015;57:e127-e132. DOI: 10.1016/j.crvasa.2015.02.005

68. Erhart P, Grond-Ginsbach C, Hakimi M, Lasitschka F, Dihlmann S, Böckler D, et al. Finite element analysis of abdominal aortic aneurysms: predicted rupture risk correlates with aortic wall histology in individual patients. J Endovasc Ther. 2014;21:556-564. DOI: 10.1583/14-4695.1

69. Martufi G, Satriano A, Moore RD, Vorp DA, Di Martino ES. Local quantification of wall thickness and intraluminal thrombus offer insight into the mechanical properties of the aneurysmal aorta. Ann Biomed Eng. 2015;43:1759-1771. DOI: 10.1007/s10439-014-1222-2

70. Hyhlik-Dürr A, Krieger T, Geisbüsch P, Kotelis D, Able T, Böckler D. Reproducibility of deriving parameters of AAA rupture risk from patient-specific 3D finite element models. J Endovasc Ther. 2011;18:289-298. DOI: 10.1583/10-3384MR.1

71. Teutelink A, Cancrinus E, van de Heuvel D, Moll F, de Vries JP. Preliminary intraobserver and interobserver variability in wall stress and rupture risk assessment of abdominal aortic aneurysms using a semi-automatic finite element model. J Vasc Surg. 2012;55:326-330. DOI: 10.1016/j.jvs.2011.08.012

72. Auer M, Gasser TC. Automatic reconstruction and finite element mesh generation of abdominal aortic aneurysms. IEEE Trans Med. Imag. 2010;29:1022-1028. DOI: 10.1109/TMI.2009.2039579

73. Xu C, Pham DL, Price JL. Image segmentation using deformable models. In: Sonka M (editor). Handbook of Medical Imaging: Medical Image Processing and Analysis. Bellingham, WA: SPIE Press; 2000. DOI: 10.1117/3.831079.ch3

74. Erhart P, Roy J, de Vries JP, Liljeqvist ML, Grond-Ginsbach C, Hyhlik-Dürr A, et al. Prediction of rupture sites in Abdominal Aortic Aneurysms after Finite Element Analysis. J Endovasc Ther. 2016;23: 115-120. DOI: 10.1177/1526602815612196

75. Brewster DC, Cronenwett JL, Hallett JW Jr, Johnston KW, Krupski WC, Matsumura JS, et al. Guidelines for the treatment of abdominal aortic aneurysms. Report of a subcommittee of the Joint Council of the American Association for Vascular Surgery and Society for Vascular Surgery. J Vasc Surg. 2003;37:1106-1117. DOI: 10.1067/mva.2003.363

76. Sakalihasan N, Michel JB. Functional imaging of atherosclerosis to advance vascular biology. Eur J Vasc Endovasc Surg. 2009;37:728-734. DOI: 10.1016/j.

ejvs.2008.12.024

77. Maier A, Essler M, Gee MW, Eckstein HH, Wall WA, Reeps C. Correlation of biomechanics to tissue reaction in aortic aneurysms assessed by finite elements and [18F]-fluorodeoxyglucose-PET/CT. Int J Numer Method Biomed Eng. 2012;28:456-471. DOI: 10.1002/cnm.1477

78. Gasser TC, Ogden RW, Holzapfel GA. Hyperelastic modelling of arterial layers with distributed collagen fibre orientations. J R Soc Lond Interface. 2006;3:15-35. DOI: 10.1098/rsif.2005.0073

79. Powell JT, Sweeting MJ, Brown LC, Gotensparre SM, Fowkes FG, Thompson SG. Systematic review and meta-analysis of growth rates of small abdominal aortic aneurysms. Br J Surg. 2011;98:609-618. DOI: 10.1002/bjs.7465

80. Sweeting MJ, Thompson SG, Brown LC, Powell JT; RESCAN collaborators. Meta-analysis of individual patient data to examine factors affecting growth and rupture of small abdominal aortic aneurysms. Br J Surg. 2012;99:655-665. DOI: 10.1002/bjs.8707

81. Richards JM, Semple SI, MacGillivray TJ, Gray C, Langrish JP, Williams M, et al. Abdominal aortic aneurysm growth predicted by uptake of ultrasmall superparamagnetic particles of iron oxide: a pilot study. Circ Cardiovasc Imaging. 2011;4:274-281. DOI: 10.1161/CIRCIMAGING.110.959866

82. Martufi G, Lindquist Liljeqvist M, Sakalihasan N, Panuccio G, Hultgren R, Roy J, et al. Local diameter, wall stress and thrombus thickness influence the local growth of abdominal aortic aneurysms. European Journal of Vascular and Endovascular Surgery. 2015;48:349. DOI: 10.1016/j.ejvs.2014.06.032

83. Roach MR, Burton AC. The reason for the shape of the distensibility curves of arteries. Can J Biochem Physiol. 1957;35:681-690. DOI: 10.1139/o57-080

84. Choke E, Cockerill G, Wilson WR, Sayed S, Dawson J, Loftus I, et al. A review of biological factors implicated in abdominal aortic aneurysm rupture. Eur J Vasc Endovasc Surg. 2005;30:227-244. DOI: 10.1016/j.ejvs.2005.03.009

85. Rizzo RJ, McCarthy WJ, Dixit SN, Lilly MP, Shively VP, Flinn WR, et al. Collagen types and matrix protein content in human abdominal aortic aneurysms. J Vasc Surg. 1989;10:365-373. DOI: 10.1016/0741-5214(89)90409-6

86. López-Candales A, Holmes DR, Liao S, Scott MJ, Wickline SA, Thompson RW. Decreased vascular smooth muscle cell density in medial degeneration of human abdominal aortic aneurysms. Am J Pathol. 1997;150:993-1007. PMID: 9060837

87. Gasser TC. Bringing vascular biomechanics into clinical practice - Simulation-based decisions for elective abdominal aortic aneurysms repair. In: Lopez CL and Peña E (editors), Patient-Specific Computational Modelling. Amsterdam, The Netherlands: Springer; 2012. DOI: 10.1007/978-94-007-4552-0_1